Spectrochimica Acta Part A 72 (2009) 474–483

Contents lists available at ScienceDirect

Spectrochimica Acta Part A: Molecular and Biomolecular Spectroscopy

journal homepage: www.elsevier.com/locate/saa

Preparation, magnetic and EPR spectral studies of copper(II) complexes of an anticancer drug analogue

E. Manoj [a], M.R. Prathapachandra Kurup [a,*], Alex Punnoose [b]

[a] Department of Applied Chemistry, Cochin University of Science and Technology, Kochi, Kerala 682022, India
[b] Department of Physics, Boise State University, Boise, ID 83725-1570, USA

ARTICLE INFO

Article history:
Received 17 June 2008
Received in revised form 30 July 2008
Accepted 17 October 2008

Keywords:
Thiocarbohydrazone
Carbohydrazone
Cu(II) complex
Dipyridyl ketone
Benzoylpyridine
Quinoline-2-carbaldehyde
Antiferromagnetism
EPR spectra

ABSTRACT

Ten new copper(II) complexes of five potential bisthiocarbohydrazone and biscarbohydrazone ligands were synthesized and physico-chemically characterized. The spectral and magnetic studies of compounds are consistent with the formation of asymmetric di-, tri- or tetranuclear copper(II) complexes of deprotonated forms of respective ligands. The variable temperature magnetic susceptibility measurements of all complexes show antiferromagnetic interactions between the Cu(II) centers, in agreement with very broad powder EPR spectra. However, frozen solution EPR spectral studies are found in contradiction with the solid-state magnetic studies and indicate that the complexes are not very stable in solutions; the possible fragmentations of complexes are found in agreement with MALDI MS results. The EPR spectral simulation of most of the compounds is in agreement with the presence of two uncoupled Cu(II) species in solution.

1. Introduction

The chemistry of multinuclear coordination metal complexes, especially of coupled systems is of special interest in various fields of science. The main reason probably is due to the phenomenon of interaction between metal centers lies at the crossover point of two widely separated areas, namely the physics of the magnetic materials and the role of polynuclear reaction sites in biological processes [1]. The EPR and magnetic studies of multinuclear Cu(II) complexes have attracted the eyes of various research groups. It is found that EPR characteristics and temperature dependence of magnetic susceptibility of multinuclear Cu(II) complexes of carbohydrazones and thiocarbohydrazones are least studied. There is only one such work reported for thiocarbohydrazone [2] and is of a dimeric dicopper(II) complex of bis(pyridine-2-aldehyde) thiocarbohydrazone, along with its crystal structure, to the best of our knowledge. The dinuclear symmetric dicopper(II) complex of bis(phenyl(2-pyridyl)methanone) thiocarbohydrazone (H_2L^2) [3] describes the X-ray structure and lacks EPR and magnetic studies. For carbohydrazones, similarly, there is only single report [4] of magnetic and EPR features discussed along with the crystal structure. The EPR characteristic of this complex is described with a powder spectrum with a broad single *g* value and magnetochemistry is confirmed with antiferromagnetic coupling between Cu(II) electrons. Therefore, an investigation including temperature dependence of magnetic susceptibility and EPR characteristics appeared relevant to the coordination chemistry of potential class of carbohydrazone and thiocarbohydrazone ligands.

The (thio)carbohydrazones are next higher homologues of potential (thio)semicarbazones, with a possible extra metal binding domain towards transition metal ions; their coordination chemistry, however, is found interesting and least studied. One of the most striking aspects of copper(II) coordination complexes is their biological activity, which is of great interest in pharmacology. Cu(II) complexes of many Schiff bases like hydrazones, semicarbazones, thiosemicarbazones, etc. have been reported to have a great variety of biological activity. In most cases, the metal complexes show more activity compared to their metal free chelating ligands. Several mono- and bis-carbohydrazone and thiocarbohydrazone ligands and some Cu(II) complexes have been synthesized and studied along with their antimicrobial and anti-mutagenic activity [5]. Thiocarbohydrazones on complexation with Cu(II) have also been proposed as anticancer drug analogues [2,6] like thiosemicarbazones and their Cu(II) complexes [7,8]. We recently

---

* Corresponding author. Tel.: +91 484 2575804; fax: +91 484 2577595.
E-mail address: mrp@cusat.ac.in (M.R.P. Kurup).

1386-1425/$ – see front matter © 2008 Elsevier B.V. All rights reserved.
doi:10.1016/j.saa.2008.10.030

have reported the first self-assembled square grid complex from a carbohydrazone ligand [9]. In continuation of our investigations on the complexing properties of carbohydrazones and thiocarbohydrazones, we synthesized the ligands 1,5-bis(di-2-pyridyl ketone) thiocarbohydrazone (H_2L^1), 1,5-bis(2-benzoylpyridine) thiocarbohydrazone (H_2L^2), 1,5-bis(quinoline-2-carbaldehyde) thiocarbohydrazone (H_2L^3), 1,5-bis(di-2-pyridyl ketone) carbohydrazone (H_2L^4) and 1,5-bis(quinoline-2-carbaldehyde) carbohydrazone (H_2L^5). We have reported the ligands H_2L^4 [10], H_2L^3 and H_2L^5 [11] recently. Also, we have reported self-assembled Ni(II) molecular square grid complexes of these ligands [12]. Here we report the syntheses and spectral characteristics of ten novel Cu(II) complexes of these five ligands with special emphasis to magnetic and EPR spectral properties.

2. Experimental

2.1. Materials

$Cu(OAc)_2\cdot H_2O$ (Qualigens), $CuBr_2$ (Merck), $CuCl_2\cdot 2H_2O$ (Merck), $Cu(ClO_4)_2\cdot 6H_2O$ (Aldrich), NaN_3 (Reidel-De Haen) were used as received and solvents methanol (Rankem), chloroform (S.D. Fine), DMF (S.D. Fine), etc. were used as received.

Caution! Perchlorate and azide complexes of metals with organic ligands are potentially explosive and should be handled with care.

2.2. Syntheses of ligands

The syntheses of ligands H_2L^1 [12], H_2L^2 [3,5], H_2L^3 [11], H_2L^4 [10] and, H_2L^5 [11] have been published earlier.

2.3. Syntheses of complexes

All the copper complexes, except $[Cu_3(HL^1)L^1Cl_3]\cdot 3H_2O$ (**1**), were synthesized by the reaction between 1:2 ratios of corresponding ligand to metal salts under neutral conditions. The complex **1** was synthesized by equimolar reaction between H_2L^1 and metal salt. Refluxing of methanolic solution of the corresponding copper salt with the methanol/chloroform solution of the ligand yielded the compound **1**, $[Cu_4(L^2)_2\cdot 2H_2O](ClO_4)_4$ (**2**), $[Cu_2(HL^2)Br_2]Br\cdot H_2O$ (**3**), $[Cu_2(HL^3)Cl_3]\cdot 2H_2O$ (**4**), $[Cu_2(HL^3)Br_2]Br\cdot H_2O$ (**5**), $[Cu_2(L^4)\cdot 2H_2O](ClO_4)_2\cdot 2H_2O$ (**7**), $[Cu_2(HL^5)Cl_3]\cdot H_2O$ (**9**) and $[Cu_2(HL^5)Br_2]Br$ (**10**), whereas compounds $[Cu_2(HL^4)Br_2]Br\cdot 3H_2O$ (**6**) and $[Cu_2L^4(N_3)_2]\cdot CH_3OH$ (**8**) were prepared in ethanol solution. The complex **8** was synthesized by the metathetical displacement of acetate ions of the metal salt by azide ions. Complexes **1** and **4** were synthesized by refluxing (10 min) 0.75 mmol of the respective ligands in 40 ml hot methanol with $Cu(ClO_4)_2\cdot 6H_2O$ in 10 ml methanol. In a similar method, complex **9** was synthesized by refluxing in 70 ml methanol for 1 h. Complexes **2** and **7** were prepared by refluxing (30 min) 0.5 mmol of the respective ligands (H_2L^2 in 10 ml chloroform and H_2L^4 in 40 ml hot methanol) with $Cu(ClO_4)_2\cdot 6H_2O$ in 10 ml methanol. Complexes **3**, **5**, **6** and **10** were synthesized by refluxing (30 min for **3** and **10**, 20 min for **5** and **6**) 0.6 mmol of the respective ligands (H_2L^2 in 10 ml chloroform, H_2L^3 and H_2L^4 in 40 ml hot methanol) with $CuBr_2$ in 10 ml methanol. For complex 8, a boiling solution of H_2L^4 (0.75 mmol in 40 ml ethanol) and $Cu(CH_3COO)_2\cdot H_2O$ (1.5 mmol) in 10 ml of ethanol was added followed by NaN_3 (1.5 mmol) in hot ethanol and refluxed for 1 h. The complexes precipitated were filtered, washed with methanol (and followed by hot water for **8**) and ether and dried *in vacuo* over P_4O_{10}.

*$[Cu_3(HL^1)L^1Cl_3]\cdot 3H_2O$ (**1**)*: Yield: 93.4%. Elemental Anal. Found (Calc.): C, 45.48 (45.10); H, 3.78 (3.21); N, 18.28 (18.29); S, 5.35 (5.24)%.

*$[Cu_4(L^2)_2\cdot 2H_2O](ClO_4)_4$ (**2**)*: Yield: 83.7%. Elemental Anal. Found (Calc.): C, 38.38 (38.57); H, 2.92 (2.59); N, 10.45 (10.79); S, 4.16 (4.12)%. Molar conductivity (Λ_M, 10^{-4} M DMF): 5 Ω^{-1} cm^2 mol^{-1}.

*$[Cu_2(HL^2)Br_2]Br\cdot H_2O$ (**3**)*: Yield: 76.3%. Elemental Anal. Found (Calc.): C, 36.00 (36.60); H, 2.14 (2.58); N, 9.96 (10.24); S, 3.66 (3.91)%. Molar conductivity (Λ_M, 10^{-3} M DMF): 88 Ω^{-1} cm^2 mol^{-1}.

*$[Cu_2(HL^3)Cl_3]\cdot 2H_2O$ (**4**)*: Yield: 88.8%. Elemental Anal. Found (Calc.): C, 39.16 (38.63); H, 3.24 (2.93); N, 12.89 (12.87); S, 5.04 (4.91)%. Molar conductivity (Λ_M, 10^{-3} M DMF): 49 Ω^{-1} cm^2 mol^{-1}.

*$[Cu_2(HL^3)Br_2]Br\cdot H_2O$ (**5**)*: Yield: 93.1%. Elemental Anal. Found (Calc.): C, 33.12 (32.83); H, 2.60 (2.23); N, 11.10 (10.94); S, 4.21 (4.17)%. Molar conductivity (Λ_M, 10^{-3} M DMF): 76 Ω^{-1} cm^2 mol^{-1}.

*$[Cu_2(HL^4)Br_2]Br\cdot 3H_2O$ (**6**)*: Yield: 50.6%. Elemental Anal. Found (Calc.): C, 32.44 (32.80); H, 2.45 (2.75); N, 13.37 (13.30)%. Molar conductivity (Λ_M, 10^{-3} M DMF): 93 Ω^{-1} cm^2 mol^{-1}.

*$[Cu_2(L^4)\cdot 2H_2O](ClO_4)_2\cdot 2H_2O$ (**7**)*: Yield: 95.3%. Elemental Anal. Found (Calc.): C, 33.86 (33.75); H, 2.57 (2.96); N, 13.78 (13.69)%. Molar conductivity (Λ_M, 10^{-3} M DMF): 164 Ω^{-1} cm^2 mol^{-1}.

*$[Cu_2L^4(N_3)_2]\cdot CH_3OH$ (**8**)*: Yield: 38.9%. Elemental Anal. Found (Calc.): C, 43.31 (43.44); H, 2.99 (3.04); N, 29.50 (29.55)%. Molar conductivity (Λ_M, 10^{-3} M DMF): 12 Ω^{-1} cm^2 mol^{-1}.

*$[Cu_2(HL^5)Cl_3]\cdot H_2O$ (**9**)*: Yield: 56.0%. Elemental Anal. Found (Calc.): C, 40.90 (40.76); H, 3.23 (2.77); N, 13.37 (13.58)%. Molar conductivity (Λ_M, 10^{-3} M DMF): 28 Ω^{-1} cm^2 mol^{-1}.

*$[Cu_2(HL^5)Br_2]Br$ (**10**)*: Yield: 48.9%. Elemental Anal. Found (Calc.): C, 34.94 (34.35); H, 2.24 (2.06); N, 11.60 (11.45)%. Molar conductivity (Λ_M, 10^{-3} M DMF): 63 Ω^{-1} cm^2 mol^{-1}.

2.4. Physical measurements

Elemental analyses of all compounds were carried out using an Elementar Vario EL III CHNS analyzer at SAIF, Kochi, India. The molar conductivities of the metal complexes in organic solvents at room temperature were measured using a direct reading conductivity meter. Electronic spectra of the ligands and their metal complexes (200–900 nm) were recorded on a Varian Cary 5000 version 1.09 UV–vis spectrophotometer. Infrared spectra of ligands and their metal complexes in the range 4000–400 cm^{-1} were recorded on a Thermo Nicolet, Avatar 370 DTGS model FT-IR spectrophotometer with KBr pellets and ATR technique at SAIF, Kochi. The far IR spectra of metal complexes were recorded using polyethylene pellets in the 500–100 cm^{-1} region on a Nicolet Magna 550 FTIR instrument at the SAIF, IIT, Bombay, India. High-resolution MALDI spectra were measured by the MS-service, Laboratorium fur Organische Chemie, ETH Zurich, Switzerland on an IonSpec HiResMALDI apparatus in a DCTB matrix and dichloromethane solvent. EPR spectra were carried out on a Bruker ElexSys E500 @9.6 GHz X band cw EPR spectrometer at EPR@ETH, ETH, Zurich, Switzerland. Variable temperature and field dependent magnetisation were carried out in *dc* mode at the Department of Physics, Boise State University, Boise, USA in the powder state on a Quantum Design PPMS superconducting magnetometer at 500 Oe field strength.

3. Results and discussion

For all complexes the respective ligands coordinate either by monodeprotonated or by dideprotonated forms under neutral conditions itself, and resulted in metal complexes with ligand to metal ratio 1:2, except for compound **1**; coordinating first Cu(II) through thiolate sulfur/enolate oxygen, azomethine N and pyridyl or quinolyl N. Azomethine N and pyridyl or quinolyl N of the remaining half of ligands and the imine nitrogen of the first half of ligand coordinate the second metal. The second copper can be coordinated by the NNS/NNO mode also to form symmetric dicopper complex through sulfur/oxygen bridging. However, for the present complexes the spectroscopic data are consistent with asymmetric dicopper complexes, as would be expected primarily, is in agreement with previous results [2,4,6]. Unfortunately, we could not get X-ray quality single crystals of any of the copper complexes for confirming the exact coordination. In the majority of cases the NNS/NNO and NNN coordination modes of (thio)carbohydrazones are seen, and the only one crystal study of a Cu(II) carbohydrazone [4] agreeing with asymmetric NNO and NNN coordination.

The complexes prepared were either green or dark brown in color. All the complexes were found to be soluble in DMF and DMSO, but only partially soluble in other organic solvents such as $CHCl_3$, ethanol, methanol, etc. The variable temperature magnetic susceptibility measurements of all complexes showed antiferromagnetic interactions between the Cu(II) centers. The complex **1** was synthesized by equimolar reaction between H_2L^1 and metal salt in methanol solution, but resulted into a product of 3:2 metal

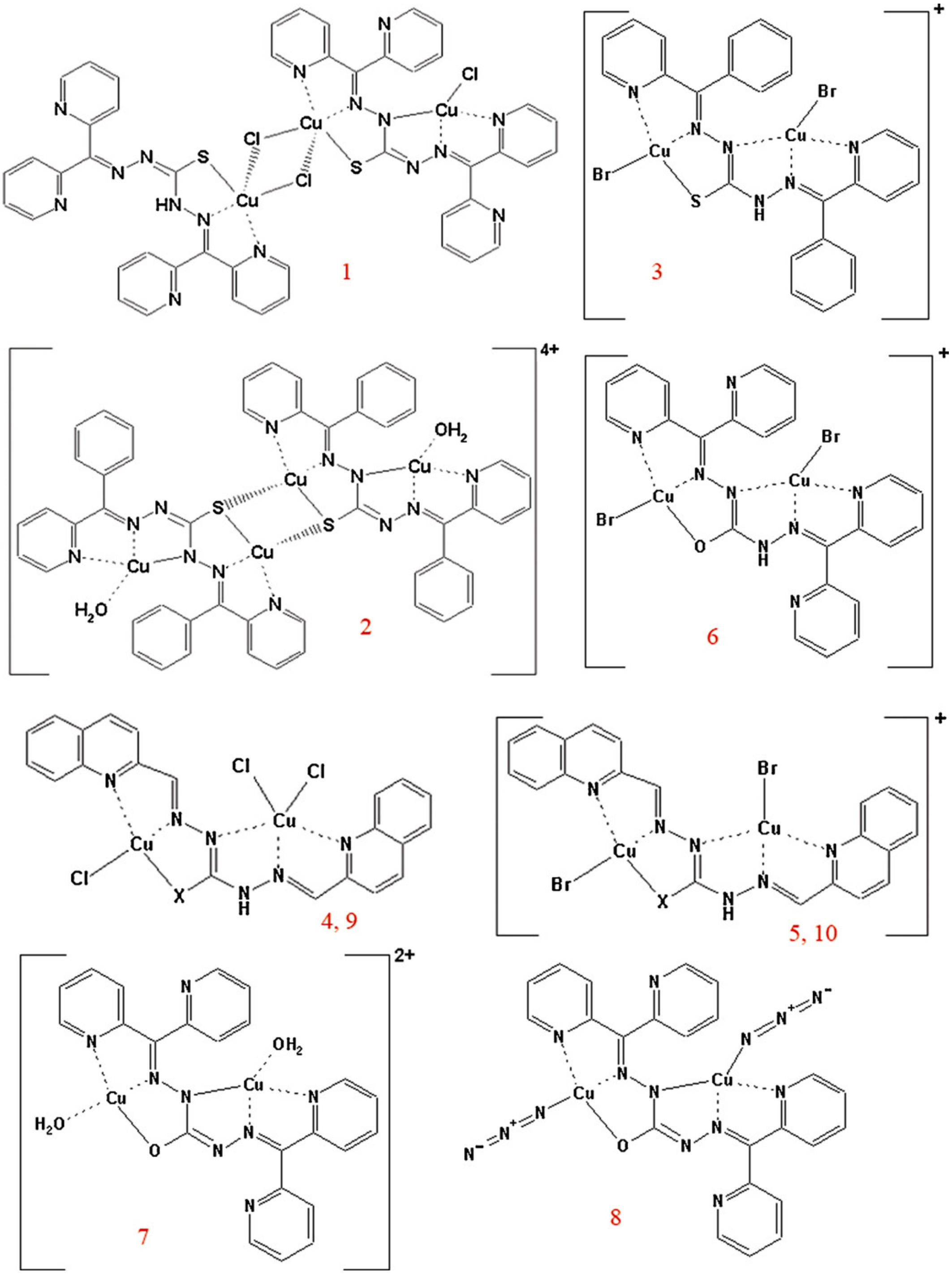

Scheme 1. The tentative structures of complexes (X = S for **4** and **5**. X = O for **9** and **10**).

ligand ratios. The molecular formula of all the Cu(II) complexes were tentatively assigned by considering spectral, magnetic and conductance studies with agreeing elemental analysis results. The tentative structures of complexes are shown in Scheme 1.

3.1. Infrared and electronic spectra

It was found that some significant changes and differences in mixing patterns of common group frequencies of complexes compared to their respective metal free ligands, attributed to ligand coordination to metal centers. Though the spectra in the IR and far IR region are rich with bands, tentative assignments of bands of Cu(II) complexes were made and are listed in Tables 1 and 2. Most of the compounds reveal a band at ~3200 cm^{-1}, along with a broad band at ~3400 cm^{-1} corresponding to the lattice water, attributed to free N–H vibrations and confirm the coordination still leaves free –NH group. For the carbohydrazone complexes absence of bands at ~1700 cm^{-1} and new ν(C–O) bands at ~1300 cm^{-1} indicate the coordination through enolate form after deprotonation. This is similar to the frequency shifts seen with the thiocarbohydrazone copper complexes **1**–**5**, where new ν(C–S) bands are seen in the range 1100–1148 cm^{-1}. Absence of bands at ~2600 cm^{-1} for thiocarbohydrazone complexes is indicative of absence of thiol tautomers in free or coordinated form in these complexes [3]. The sulfur coordination is supported by the evidences of strong bands seen in the range 320–349 cm^{-1} assigned to ν(Cu–S) for complexes **1**–**5**, while for complexes **6**–**10** oxygen coordination is clear as the presence of strong bands in the range 344–390 cm^{-1} of ν(Cu–O) [13]. The differences in mixing patterns of C=N and N–N groups of complexes compared to their respective metal free ligands may be attributed to possible azomethine coordination. Also, the bands in the range 408–425 cm^{-1}, assigned to the $\nu(\mathrm{Cu–N_{azo}})$ band [14] also support the azomethine nitrogen coordination in all complexes. The pyridyl or quinolyl coordination is supported by the bands in the range 255–298 cm^{-1}, consistent with the $\nu(\mathrm{Cu–N_{py}})$ [15]. However it is not possible to confirm the position of coordination explicitly from IR results alone.

The perchlorate complex **2** shows strong bands at 1100 and 626 cm^{-1}, while complex **7** exhibits broad bands at 1060–1140 and strong bands at 623 cm^{-1} indicating the presence of ionic perchlorate. The bands at ~1100 cm^{-1} are assignable to $\nu_3(\mathrm{ClO_4})$ and the unsplit bands at ~625 cm^{-1} assigned to $\nu_4(\mathrm{ClO_4})$. For both the compounds, very weak bands at 938 cm^{-1} may be due to $\nu_1(\mathrm{ClO_4})$ suggesting that ionic perchlorate is distorted from tetrahedral symmetry possibly due to lattice effects or hydrogen bonding by the NH functions of the coordinated ligand [16]. This along with unsplit ν_3 and ν_4 bands show exclusive presence of non-coordinated perchlorate group [17]. For the azido complex **8**, a broad band at 2051 is assigned as asymmetric stretching of coordinated azido group [14]. The broadness may be due to the presence of second azide group. A strong band at 1240 cm^{-1} may be attributed to symmetric stretching band of coordinated azido groups. Also the weak band at 640 cm^{-1} may be of δ(NNN). The far IR spectrum also supports this assignment as the $\nu(\mathrm{Cu–N_{azide}})$ vibration is seen at 420 cm^{-1}.

The far IR spectra of complexes are found interesting and worth to support the metal ligand coordination modes. The spectrum of compound **1** shows strong bands at 320 and 161 cm^{-1}, due to ν(Cu–Cl) terminal and bridging modes respectively [17–19], indicating bridging character in the Cu–Cl bond. However for the other chloro compounds **4** and **9** only terminal ν(Cu–Cl) band is observed at 304 and 329 cm^{-1} respectively. No bands at ~160 cm^{-1} corresponding to the bridging ν(Cu–Cl) are found for these complexes. The ν(Cu–Br) frequency of complexes **5**, **6** and **10** are observed at 240 cm^{-1}, while that of complex **3** is seen at 238 cm^{-1}, consistent with the terminal bromo ligand [14,18,19].

Table 1
IR spectral assignments of ligands and their Cu(II) complexes (cm^{-1}).

Compounds	νH_2O	νN–H	νC=N+ νC=C	νC–N/νheterocyclic	νC=O/νC–O	νC=S/νC–S	νN–N
H_2L^1		3340br	1580m, 1483s, 1454vs, 1423s	1303m, 1282m		1223s	1117s
H_2L^2		3323m, 3266m	1568s, 1495vs, 1459vs, 1422s	1358m, 1300s		1225vs	1132vs
H_2L^3		3442br	1616m, 1575s, 1542m, 1482vs, 1412vs	1335m, 1293s		1209s	1126s
H_2L^4		3428br, 3155m	1580m, 1491s, 1456s, 1426s	1324s, 1279m	1704vs		1127vs
H_2L^5		3455br	1593m, 1533vs, 1501s, 1454m, 1431m	1329m, 1264s	1696vs		1126s
$[Cu_3(HL^1)L^1Cl_3]\cdot 3H_2O$ (**1**)	3409br	3229sh	1583m, 1488s, 1455vs, 1422vs	1385s, 1282s		1100s	1236m, 1153m
$[Cu_4L^2{}_2)\cdot 2H_2O](ClO_4)_4$ (**2**)	3424br		1593s, 1493m, 1467s, 1407vs	1318s, 1296s		1142s	1207s
$[Cu_2(HL^2)Br_2]Br\cdot H_2O$ (**3**)	3338m	3581m	1591s, 1561vs, 1529s, 1466s, 1438s, 1410m	1330m, 1300s		1100s	1200m, 1152m
$[Cu_2(HL^3)Cl_3]\cdot 2H_2O$ (**4**)	3440br	3205sh	1585m, 1550m, 1510m, 1470m	1377m, 1315vs, 1251s		1148vs	1218vs, 1088s
$[Cu_2(HL^3)Br_2]Br\cdot H_2O$ (**5**)	3436br	–	1618m, 1591s, 1552m, 1464s, 1413vs	1332vs, 1251m		1148vs	1215s, 1083s
$[Cu_2(HL^4)Br_2]Br\cdot 3H_2O$ (**6**)	3412br	3252sh	1602vs, 1567s, 1511s, 1474s, 1427s	1361s, 1237s	1307vs		1174m, 1124s
$[Cu_2(L^4)\cdot 2H_2O](ClO_4)_2\cdot 2H_2O$ (**7**)	3421br		1597s, 1564s, 1514vs, 1464s	1371s, 1270s	1311vs		1240s
$[Cu_2L^4(N_3)_2]\cdot CH_3OH$ (**8**)			1593s, 1561s, 1498s, 1450s	1357m, 1336m	1285s		1172m, 1126s
$[Cu_2(HL^5)Cl_3]\cdot H_2O$ (**9**)	3414br	3207sh	1615m, 1583s, 1547m, 1512s, 1483s, 1448m	1385vs, 1345m	1296s		1245m, 1140vs
$[Cu_2(HL^5)Br_2]Br$ (**10**)		3432br, 3212sh	1605m, 1585vs, 1540m, 1515s, 1476s, 1445m	1378vs, 1355m	1294s		1240s, 1142vs

br = broad, sh = shoulder, s = strong, vs = very strong, m = medium and w = weak.

Table 2
Metal–ligand stretching frequencies (cm^{-1}) of the complexes.

Compounds	νCu–N_{azo}	νCu–N_{py}/qu	νCu–S	νCu–O	νCu–X
1	409s	267s	337s		320s, 161s
2	415s	270s	320s		
3	410s	270s	340m		238s
4	408m	264m	349s		304m
5	411m	298s	349s		240s
6	417s	274s		344s	240s
7	415m	280m		379m	
8	403s	259s		370s	
9	405m	255m		380m	329m
10	425s	275s		390s	240s

X = Cl for **1**, **4** and **9**. X = Br for **3**, **5**, **6** and **10**.

The electronic spectra of carbohydrazone Cu(II) complexes (**6**–**10**) differ considerably from that of thiocarbohydrazone Cu(II) complexes (**1**–**5**). The absorption bands with extinction coefficients are listed in Table 3. The intense bands at ~20,000 cm^{-1} of thiocarbohydrazone Cu(II) complexes mainly include S → Cu charge transfer transitions and possible $^2E_1 \leftarrow {}^2B_1$ *d*–*d* bands, which tails to ~17,000 cm^{-1}. Due to broadness of the bands, all possible *d*–*d* transitions could not be resolved. For the Cu(II) complexes, with a square-based pyramid geometry in a close to C_{4v} group, there are three spin allowed transitions viz. $^2A_1 \leftarrow {}^2B_1$, $^2B_2 \leftarrow {}^2B_1$ and $^2E_1 \leftarrow {}^2B_1$, usually very difficult to resolve them into separate bands due to the very low energy difference between these bands. For a square planar geometry with $d_{x^2-y^2}$ ground state, similar transitions are possible corresponding to $d_{x^2-y^2} \rightarrow d_{z^2}$, $d_{x^2-y^2} \rightarrow d_{xy}$ and $d_{x^2-y^2} \rightarrow d_{xz}; d_{yz}$. However, we could not resolve these low intense bands. EPR studies are found very consistent with a $d_{x^2-y^2}$ ground state and is the most common ground state for Cu(II) complexes. For carbohydrazone Cu(II) compounds intense bands at ~21,000 cm^{-1} are attributed to O → Cu charge transfer transitions. The intense bands near 27,000 cm^{-1} are attributed to N → Cu charge transfer transitions and are seen for all complexes. The bands at ~44,000 and ~32,000 cm^{-1} are assigned as intraligand $\pi \rightarrow \pi^*$ and $n \rightarrow \pi^*$ transitions of complexes, suffered marginal shift from that of their corresponding free ligands. However some charge transfer bands may also be present in this region for Cu(II) complexes [20]. Also, many intraligand transitions are observed in complexes with quinoline-derived ligands, as expected. As the quinoline is an electron delocalizing group, some of the bands may be metal to ligand charge transfer bands, though which are difficult to assign.

Table 3
Electronic spectral features of Cu(II) complexes.

Compounds	Absorbance features λ_{max} (cm^{-1}) (ε (M^{-1} cm^{-1}))
1	45,660, 37,170, 30,770, 24,690sh, 22,075, 19,010sh
2	36,500 (8900), 29,760 (6560), 21,830sh (8100), 18,940 (10,760)
3	35,970 (18,370), 29,070 (15,500), 27,100sh (13,090), 20,640sh (21,120), 18,730 (24,930)
4	33,560sh (14,950), 31,850 (15,010), 26,180 (13,270), 20,580 (14,970), 18,940sh (13,090)
5	32,360 (17,040), 26,110 (12,440), 22,730sh (13,810), 20,700 (16,280), 19,050sh (14,390)
6	32,470 (22,410), 30,900 (22,080), 26,380sh (4820), 20,920 (8450)
7	30,390sh (21,050), 27,470sh (14,880), 20,920 (21,550)
8	33,220sh (19,400), 30,390sh (15,980), 26,320 (14,010), 20,660 (136,20)
9	32,150 (20,470), 29,940sh (13,640), 26,500 (9720), 25,250 (10,190), 24,150 (10,600), 20,040 (19,670)
10	32,890 (23,230), 29,940sh (16,630), 26,670 (13,470), 25,250 (13,910), 23,810sh (14,180), 21,100 (20,940), 20,040sh (18,580)

All spectra, except that of complex **1**, were recorded as DMF solution. Spectrum of **1** was taken in ethanol solution.

3.2. *Magnetic studies*

For all the copper compounds the temperature dependence of molar magnetic susceptibility χ_m in the powder form is carried out in the temperature range 5–325 K. All compounds are found to show common features. The effective magnetic moments μ_{eff} at room temperature of all dicopper(II) compounds are found to be low or near compared to that expected for two independent Cu(II) ions (2.45μ_B) and also show a regular decrease with decreasing temperature suggesting antiferromagnetic interactions between Cu(II) ions. The temperature dependence curves of **1** and **2** also show similar nature. These features indicate a dominant antiferromagnetic interaction in these compounds. Also it is found that Curie law is not obeyed by all systems, in agreement with the exchange coupling.

The room temperature μ_{eff} of trinuclear complex **1** and tetranuclear complex **2** are found to be 3.09 and 3.60μ_B respectively, and as the temperature is lowered μ_{eff} decreases gradually and reaches a minimum of 0.53μ_B for **1** and 0.47μ_B for **2** at 5 K. Both compounds show dominant antiferromagnetic interactions as evidenced by the behavior of variable temperature magnetic curves. The slightly higher μ_{eff} value at room temperature for **1** (by 3%) and **2** (by 4%) compared to spin only magnetic moments for three and four independent Cu(II) species respectively may be attributed to the presence of orbital contribution or presence of impurities.

For all the other complexes, the room temperature effective magnetic moments μ_{eff} range from 1.83 to 2.44μ_B. The values include 2.2, 1.90, 2.44, 2.09, 2.13, 1.83, 2.03 and 1.98μ_B respectively at room temperature and show minima of 0.29, 0.30, 0.31, 0.40, 0.28, 0.24, 0.26 and 0.26μ_B at 5 K respectively for complexes **3**, **4**, **5**, **6**, **7**, **8**, **9** and **10** respectively. The thermal dependence curves of μ_{eff} of all these complexes are almost similar and show a regular decrease on cooling, which suggest strong antiferromagnetic interactions between the Cu(II) centers. The experimental temperature dependence curves of molar magnetic susceptibility χ_m and effective magnetic moments μ_{eff} of some selected complexes are given in Figs. 1–5. The general nature of the susceptibility curves of all complexes are consistent with strong coupling interactions between Cu(II) electrons through their connecting moiety. The rapid increase in χ_m for some compounds at low temperature is due to monomer impurity.

The model often used to describe the magnetic behavior of isolated dicopper(II) complexes is provided by modified Bleaney–Bowers equation [21]. The susceptibility data of all dicopper complexes, however, found cannot be satisfactorily fitted to Bleaney–Bower equation. Around the maximum, the fit departs from the experimental data. Inter-dimer exchange interactions between neighboring ions may occur [22], possibly having influence in the susceptibility around T_{max}. The existence of other kinds of secondary interactions may also be present in the compounds.

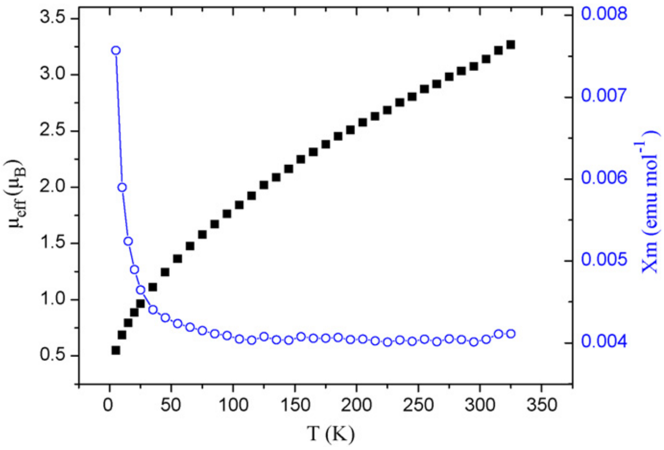

Fig. 1. Temperature dependence of effective magnetic moment μ_{eff} (■) and of molar magnetic susceptibility χ_{m} (○) of complex **1**.

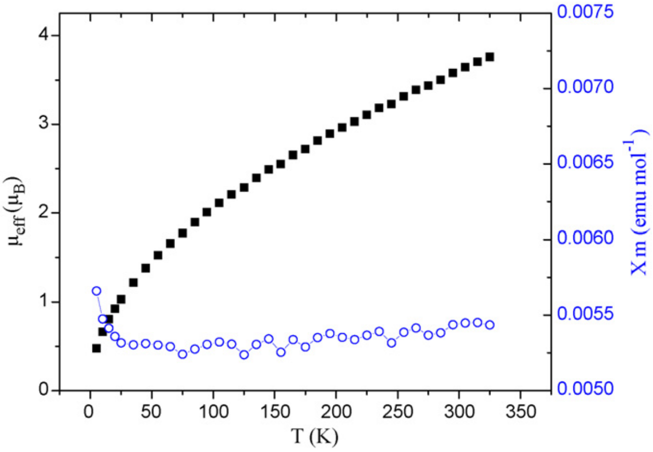

Fig. 2. Effective magnetic moment μ_{eff} (■) and molar magnetic susceptibility χ_{m} (○) data as a function of temperature for complex **2**.

To fit and interpret the magnetic susceptibility data of complexes, first it is necessary to find all possible magnetic pathways in the complex structures, and in the absence of X-ray crystallographic structural results it is not possible to use any magnetic interacting models.

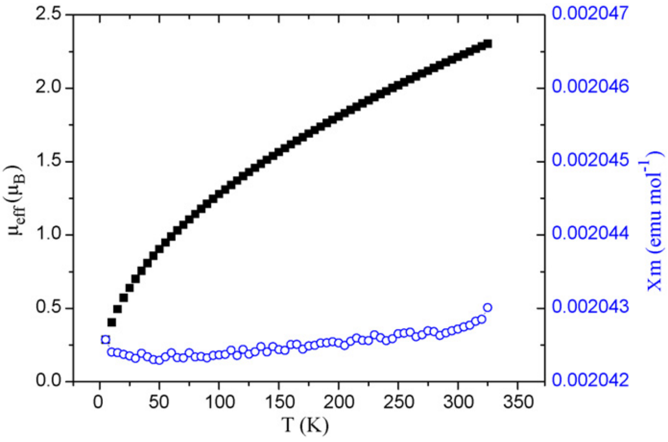

Fig. 3. Effective magnetic moment μ_{eff} (■) and molar magnetic susceptibility χ_{m} (○) data as a function of temperature for complex **3**.

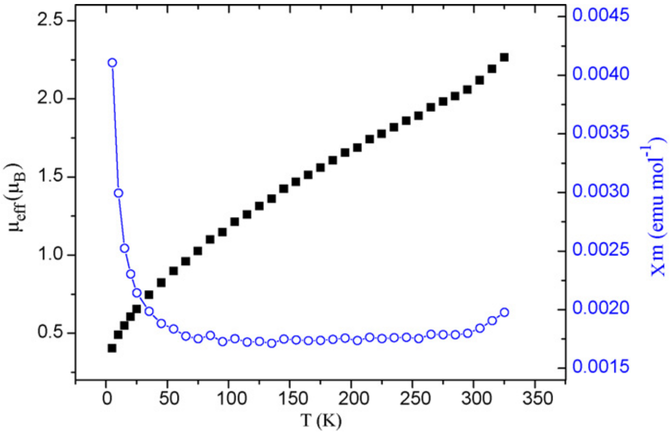

Fig. 4. Effective magnetic moment μ_{eff} (■) and molar magnetic susceptibility χ_{m} (○) data as a function of temperature for complex **6**.

3.3. MALDI spectral studies

MALDI mass spectra of all the complexes were taken in CH_2Cl_2 as DCTB mix on positive ion mode. The MALDI mass spectra of Cu(II) complexes show some similar features. Though molecular ions could not be observed for all compounds, sensible fragments were observed. This is reasonable as the structure and stability of coordination complexes under ionization conditions are dependent on various factors like the ligand itself, metal ions, counter ions, solvent, temperature, concentration, etc. However, the $[Cu(HL)]^+$ fragment was readily observed in all cases.

The complex **1** exhibits peaks centered at *m*/*z* 501.1, 467.1, 445.2, 405.2, etc. The peak at 501.1 assigned as $[Cu(HL^1)]^+$ (calc. 500) and at 467.1 as $[Cu(HL^1)–SH]^+$ (calc. 468) agreeing with calculated isotopic distribution patterns. The compound **2** shows peaks centered at *m*/*z* 1219, 1123, 1061, 998, 935, 561, 499, etc. (Fig. 6). The very low intense peak at 1219 may be of the species $[Cu_4L^2{}_2(ClO_4)–2H^+]^+$ (calc. 1220). Other major peaks are assigned as $[Cu_2L^2(HL^2)·CH_3OH·H_2O]^+$ (calc. 1061), $[Cu_2L^2(HL^2)]^+$ (calc. 997), $[Cu(H_2L^2)HL^2]^+$ (calc. 934), $[Cu_2L^2–H^+]^+$ (calc. 559). The base peak corresponds to $[Cu(HL^2)]^+$ (calc. 498). All these are in agreement with calculated isotopic patterns and are characteristic peaks for the compound which is assigned as molecular formula $[Cu_4L^2{}_2·2H_2O](ClO_4)_4$.

The peaks of **3** are seen centered at *m*/*z* 641.8, 560.9 and base peak at 498, which are assigned as $[Cu_2L^2Br]^+$ (calc. 641),

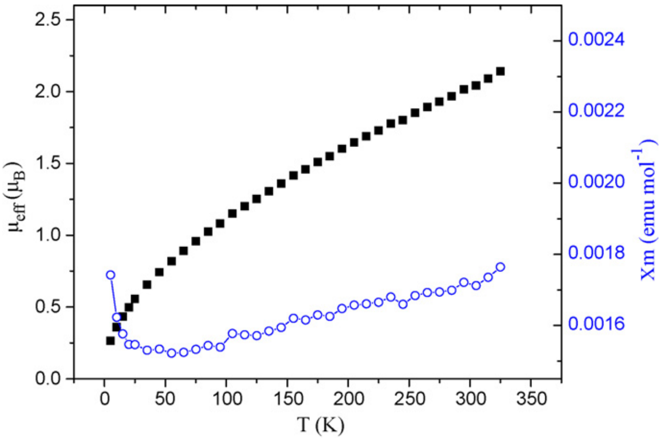

Fig. 5. Effective magnetic moment μ_{eff} (■) and molar magnetic susceptibility χ_{m} (○) data as a function of temperature for complex **9**.

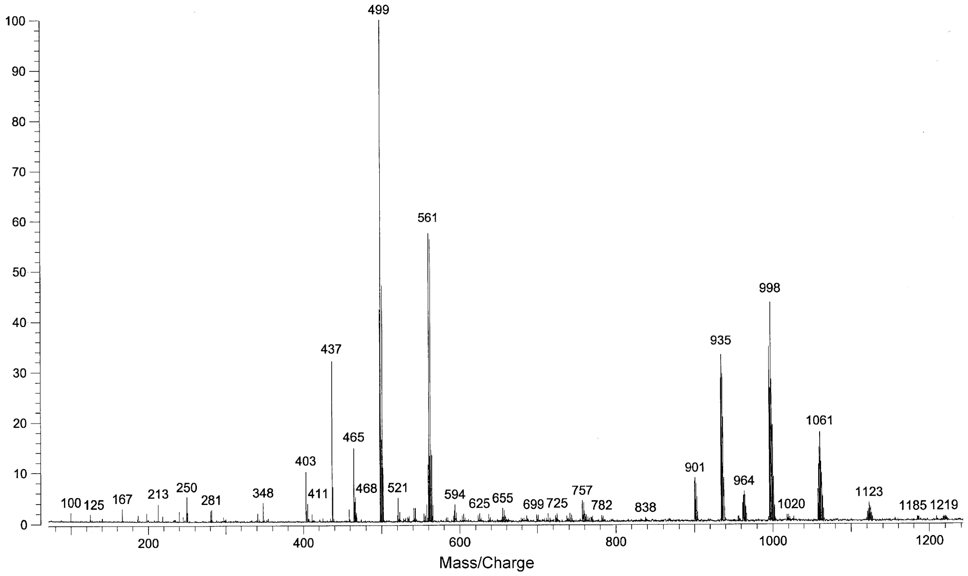

Fig. 6. The MALDI MS spectrum of tetranuclear copper(II) compound **2**.

$[Cu_2L^2–H^+]^+$ (calc. 559) and $[Cu(HL^2)]^+$ (calc. 498) are in well agreement with simulation. Of the other weaker peaks, *m*/*z* 785.6 corresponds to $[Cu_3L^2Br_2–H^+]^+$ (calc. 784) may be formed under ionization condition by the coordination of one copper to the species $[Cu_2L^2Br]^+$. The spectrum of complex **4** exhibits peaks centered at *m*/*z* 831, 447, 385, etc. The peak at 447 corresponds to $[Cu(HL^3)]^+$ (calc. 446) and is in agreement with calculated isotopic distribution. The base peak at 385 is of the free ligand H_2L^3 and weaker peak at 831 is assigned as $[Cu(HL^3)(H_2L^3)]^+$ (calc. 830), may be formed under MALDI conditions. The spectrum of **5** shows *m*/*z* 447 as base peak, which corresponds to $[Cu(HL^3)]^+$ (calc. 446) and the peak at 413 corresponds to $[Cu(HL^3)–SH]^+$ (calc. 414), both are in agreement with calculated isotopic patterns. The spectra of complexes **6**–**8** are found not good enough to get characteristic peaks. A weak peak centered at 567 is assigned to $[Cu(H_2L^4)Br]^+$ (calc. 566) for compound **6**. The base peak of **9** and **10** at *m*/*z* 369 are of the free ligand H_2L^5. The spectrum of **9** exhibits a characteristic peak at 431 of $[Cu(HL^5)]^+$ (calc. 430) and a new coordinated species at 799 of $[Cu(HL^5)(H_2L^5)]^+$ (calc. 798) as weaker peak. These results are attributed to the less stability of these carbohydrazone copper complexes in solution and/or under the condition of MALDI.

3.4. EPR spectral studies

The EPR spectra of all compounds under the investigation condition, in frozen DMF solutions at 77 K, exhibit signals characteristics of uncoupled Cu(II) species at ~3300 G and not showed signals typical for coupled binuclear complexes. The binuclear complex is connected with the antiferromagnetic coupling of two Cu(II) ions, leading to a singlet ground state and an excited spin triplet state. For a coupled system of two Cu(II) species equally distributed seven hyperfine features ($2nI+1$; $n=2$ and $I=3/2$) are expected. However none of the frozen solution spectra show this feature and half field signals, and the computer simulation of most of the compounds is in good agreement with the presence of two uncoupled Cu(II) species. This frozen DMF features are in contradiction with the solid-state magnetic studies, which is attributed to the possible fragmentation in DMF at low concentrations. Absence of any half field signals in solution for all the compounds may be due to the absence of any considerable Cu–Cu interactions, which might be due to the lack of enough intensity. It is most likely due to the dissociation of di- or polynuclear to mononuclear copper compounds and presence of an equilibrium mixture with greater monomer percentage. The EPR spectra of binuclear compounds are reported to dissociate to yield a series of mononuclear species, depending upon concentration [23].

The copper(II) ion, with a $3d^9$ configuration, has an effective spin of $S=1/2$ and is associated with a spin angular momentum, $m_s=\pm 1/2$, leading to a doubly degenerate spin state in the absence of a magnetic field. In a magnetic field the degeneracy is lifted between these states and the energy difference between them is given by $E=h\nu=g\beta B$, where h is Planck's constant, ν is the frequency, g is the Lande splitting factor (equal to 2.0023 for a free electron), β is the Bohr magneton and B is the magnetic field. The appropriate axially symmetric spin Hamiltonian [24,25] is then given by

$$\hat{H}=g_{\|}\beta B_zS_z+g_{\perp}\beta(B_xS_x+B_yS_y)+A_{\|}S_zI_z+A_{\perp}(S_xI_x+S_yI_y) \quad (1)$$

The formation of a binuclear complex is connected with the antiferromagnetic coupling of two Cu(II) ions, leading to a singlet ground state and an excited spin triplet state. The energy difference, $2J$, between these states depends on the strength of the interaction. If the triplet state is thermally accessible ($2J \sim kT \sim 200–400\,\text{cm}^{-1}$), paramagnetism is observed and the EPR spectra could be satisfactorily described using the interactive spin Hamiltonian [26] for isolated Cu(II) dimer ($S=1$),

$$\hat{H}=g\beta BS+DS_z^2+E(S_x^2-S_y^2)-\frac{2D}{3} \quad (2)$$

where D and E are the zero field splitting parameters.

However, the present spectra all indicate the presence of two different Cu(II) species and there are no characteristic features of transfer of any coupling between the two Cu(II) centers by the bridging moiety connecting them in frozen DMF. So the spectra were simulated by considering with the presence of two noninteracting Cu(II) d^9 groups using EasySpin [27]. The various magnetic interaction parameters obtained by simulations are summarized in Table 4.

The spectra of all the compounds, except **7**, exhibit some common features as evidenced by the nature of spectra. The spectrum of **7** is broad but not isotropic in nature and does not give much information, but is consistent with antiferromagnetic interaction between Cu(II) centers, as it is expected. The experimental and simulated best fits of selected complexes are given in Figs. 7–10. All of

Table 4
EPR spectral parameters of the copper(II) complexes in frozen DMF solution.

Compounds	Species	$g_{\|\|}$	$g_{\perp}$	$A_{\|\|}$ (Cu) cm^{-1} (10^{-4})	$A_{\perp}$ (Cu) cm^{-1} (10^{-4})	G	Species g_{av}	g_{av}	α^2	f
1	A	2.226	2.049	175.12	20.01	4.79	2.108	2.1	0.7702	127.11
	B	2.186	2.045	166.78	18.35	4.30	2.092		0.7052	131.07
2	A	2.185	2.061	191.79	25.01	3.11	2.102	2.145	0.7806	113.93
	B	2.391	2.085	135.09	13.34	4.70	2.187		0.8394	176.99
3	A	2.392	2.085	133.43	10.01	4.71	2.187	2.185	0.8358	179.27
	B	2.392	2.078	133.43	10.01	5.14	2.183		0.8328	179.27
4	A	2.392	2.080	133.43	13.34	5.01	2.184	2.144	0.8336	179.27
	B	2.147	2.082	120.08	10.01	1.81	2.104		0.5524	178.79
5	A	2.391	2.080	133.43	10.01	5.00	2.184	2.137	0.8326	179.19
	B	2.123	2.074	113.41	8.34	1.68	2.090		0.5066	187.19
6	A	2.310	2.075	163.45	16.68	4.23	2.153	2.142	0.8329	141.33
	B	2.254	2.070	176.79	20.01	3.72	2.131		0.8117	127.49
7		2.0955								
8	A	2.257	2.054	145.1	16.68	4.93	2.122	2.121	0.7199	155.55
	B	2.244	2.050	173.45	26.68	5.07	2.119		0.7839	129.37
9	A	2.392	2.0801	133.43	10.01	5.01	2.184	2.175	0.8337	179.27
	B	2.352	2.0711	146.77	13.34	5.08	2.165		0.8269	160.25
10	A	2.391	2.0845	135.09	6.67	4.73	2.187	2.179	0.8391	176.99
	B	2.352	2.0803	146.77	8.34	4.48	2.171		0.8308	160.25

these spectra are found axial in nature and $g_{||} > g_{\perp} > 2.0023$ for both species considered, which points towards a $d_{x^2-y^2}$ ground state [28].

The geometric parameter G, empirical factor f and in-plane sigma bonding parameter α^2 values of all simulated spectra are calculated. G is a measure of the exchange interaction between the copper centers, is calculated for each species using the equation: $G = (g_{||} - 2.0023)/(g_{\perp} - 2.0023)$ for all axial spectra. If $G > 4$, exchange interaction is negligible and if it is less than 4, considerable exchange interaction is indicated in the solid complex [29]. The value of in-plane sigma bonding parameter α^2 was estimated for each species, from the expression,

$$\alpha^2 = -\frac{A_{||}}{0.036} + (g_{||} - 2.0023) + \frac{3}{7}(g_{\perp} - 2.0023) + 0.04$$

The empirical factor f, an index of tetragonal distortion, is calculated as $f = g_{||}/A_{||}$.

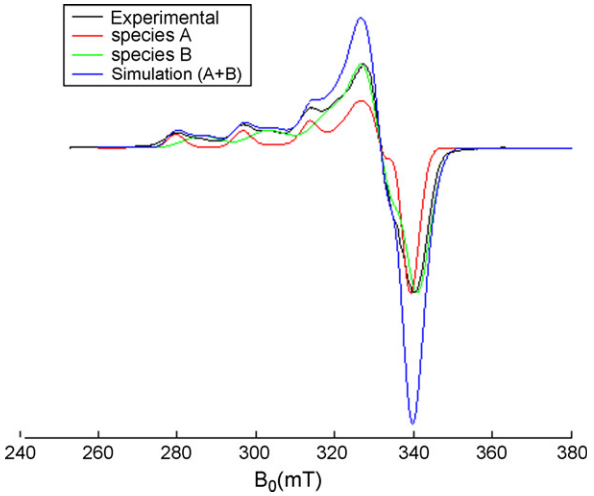

Fig. 7. Experimental (black) and simulated best fit (blue) of the frozen DMF EPR spectrum of complex **1**. (For interpretation of the references to color in this figure legend, the reader is referred to the web version of the article.)

It has been suggested that the smaller value of $A_{||}$ arises from a distortion of a copper site away from planarity [30]. The hyperfine splittings are more or less twice than that for dimers indicating the complex under investigation behaves like localized electrons [28] in each copper(II) centers. The value of $A_{||} < 0.0140\,\mathrm{cm}^{-1}$ rules out the possibility of square planar nature for such Cu(II) centers as such values are not reported for any complexes even with four sulfur ligands [31]. The empirical factor f is an index of tetrahedral distortion and its value vary from 105 to 135 for small to extreme distortion in square planar complexes, and that depends on the nature of the coordinated atom [32]. Here the f values of some of the complexes are indicating significant distortion from planarity. The value of f can increases markedly on the introduction of tetrahedral distortion to the chromophore. The tetrahedral distortion of a square planar chromophore with any of the biomimetic (N, O or S) donors reduces $A_{||}$ and increases $g_{||}$, shifting the f values [31]. The factor α^2 is a covalency parameter, which describes the in-plane sigma bonding, arises from the dipole–dipole interaction between magnetic moments associated with the spin motion of

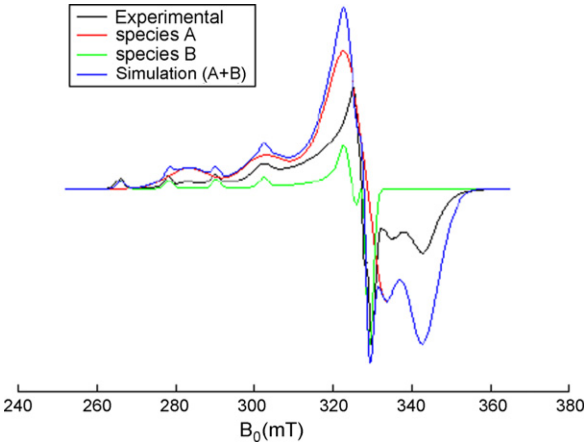

Fig. 8. Experimental (black) and simulated best fit (blue) of the frozen DMF EPR spectrum of complex **2**. (For interpretation of the references to color in this figure legend, the reader is referred to the web version of the article.)

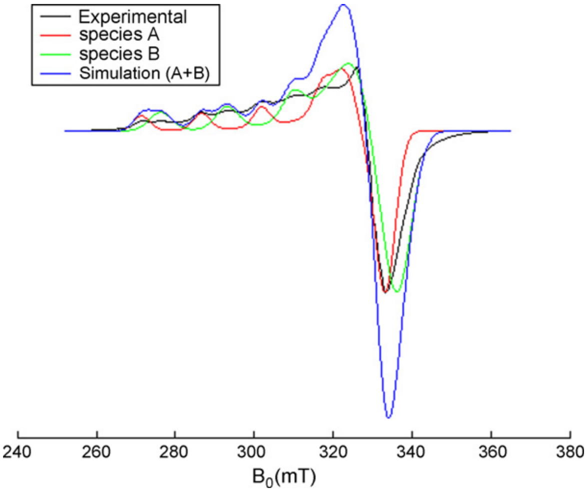

Fig. 9. Experimental (black) and simulated best fit (blue) of the frozen DMF EPR spectrum of complex **6**. (For interpretation of the references to color in this figure legend, the reader is referred to the web version of the article.)

the electron and the nucleus and its value decreases with increasing covalency [33]. The stronger covalency should result in smaller hyperfine interaction. Since, α^2 values obtained lies above 0.5 and below 1.0, which is expected for 100% ionic character of the bonds and become smaller with increasing covalent bonding, it is inferred that the complexes have some covalent character in the ligand environment. The values of α^2 indicate that approximately 80% of the spin population is in the copper $d_{x^2-y^2}$ orbital of most of the Cu(II) species concerned.

The spectrum of compound **1** shows an axial nature with the indication of a second Cu(II) species as evidenced in the spectrum, there was hardly any indications of a third species. Both two species of the complex **1** show typical axial behavior with different $g_{||}$ and $g_\perp$values. $g_{||} > g_\perp > 2.0023$ are consistent with a $d_{x^2-y^2}$ ground state in a square planar or square pyramidal geometry. The *f* values obtained are nearly the same as reported for similar chloro-bridged copper(II) dimers [22]. The spectrum of the compound **2** is found to be more of an axial type. The simulation was done by considering two uncoupled axial Cu(II) species, though the second Cu(II) species might be of rhombic features. There may be more than two different species also. However, the simulation is found in good agreement with two axial Cu(II) species.

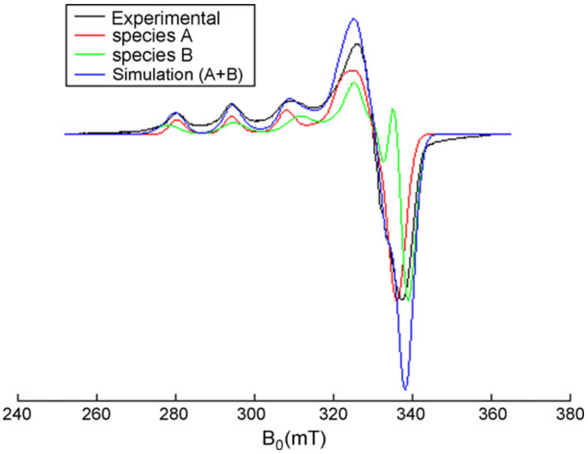

Fig. 10. Experimental (black) and simulated best fit (blue) of the frozen DMF EPR spectrum of complex **8**. (For interpretation of the references to color in this figure legend, the reader is referred to the web version of the article.)

The spectrum of compound **3** resembles a typical axial Cu(II) monomeric species. However, as the complex is having two metal centers, the simulation was done by considering so. However, fragmentation due to lower stability in DMF can also lead to spectra like this (high $g_{||}$ values). But, the EPR of the copper is governed by the chemical nature and charge state of the close-lying ligand atoms to the metal atom and is not directly correlated with thermodynamic parameters, which govern stability of metal–ligand complexes [30]. For example, various polyamines bind to copper with first dissociation constants ranging over 16 orders of magnitude while the EPR parameters do not vary significantly [30]. Thus, arguments based on stability alone could not be used to make the type of assignment [30]. Also it is reported that, on the whole, EPR studies even of frozen solutions of a wide range of copper(II) systems, do not show any evidence of pair formation, though EPR triplet spectra had been observed in a number of copper compounds [34]. The spectra of compounds **4** and **5** show common features. The axial spectra show the presence of second uncoupled Cu(II) species. The two different species present in **4** resembles that in **5** as evidenced by the $g_{||}$ and $g_\perp$ values of the two species A and B. Both complexes have a similar Cu(II) center as evidenced by an exactly matching parameters of one of their Cu(II) species (species A).

The $g_{||}$ values of some of the species in these compounds are too high than expected, is attributed to weak coordination to metal centers [30]. The electron-donating capacity of a ligand to Cu(II) will determine the magnitude of $g_{||}$. The presence of electron poor water ligation can also be behind the high $g_{||}$ values, for example. The very low $A_{||}$ values also support this. These high $g_{||}$ values expect a positive net charge for the complex part. So the possibility of ionic copper at NNN centers and its weakening may be behind this and is in accordance with thiolato/enolato coordination assigned to second Cu(II) for **4**, **5**, **9** and **10**. For complexes having the same atoms of ligation, a decrease in charge of the metal–ligand complex decreases $g_{||}$ and increases $A_{||}$ [30]. Conversely, the smaller *g* values for some other species indicate increased delocalization of the unpaired spin density away from the copper nucleus, and has been often interpreted in terms of increased covalency in the metal–ligand bond [35,36]. In all the complexes having different Cu(II) species $g_{||} > g_\perp > 2.0023$ and *G* values within the range 1.68–5.14 are consistent with a $d_{x^2-y^2}$ ground state in a square planar or square pyramidal geometry, as would be expected, and rules out the possibility of a trigonal bipyramidal structure which would be expected to have $g_\perp > g_{||}$. Octahedral geometry is rarely sustained in Cu(II) complexes as they are most prone to Jahn Teller distortion giving rise to rhombic symmetries. Also, it is inferred that the geometry of the compound undergoes changes upon dissolution in polar coordinating solvents.

The compounds **4**, **5**, **9** and **10** having quinolyl substituted ligands have one similar Cu(II) species as evidenced by the nearly the same $g_{||}$ values, may be indicating a weaker N,N,N coordination. The second species in **4** and **5** are almost same and smaller $g_{||}$ values may be due to possible NNS coordination compared to the possible N, N, O coordination in **9** and **10**. The $g_{||}$ values of both Cu(II) species in compounds **1**, **6** and **8** having dipyridyl substituted ligands are different from the above complexes may support this. However this observation is ambiguous, especially without confirming the exact nature of the complexes in solution and in the absence of any crystal structure to support the coordination.

The room temperature powder EPR spectra of complexes are very broad with no good hyperfine splittings. These kinds of spectra do not give much information but indicates the presence of antiferromagnetic interaction between copper(II) ions. Some of the powder spectra however exhibit some indications of very weak triplet state lines at half fields of Cu(II)...Cu(II) interactions. A previous report [2] of a similar asymmetric Cu(II) compound of bis(pyridine-2-aldehyde) thiocarbohydrazone in frozen H_3PO_4 solution shows two monomeric axial Cu(II) species, one with a $g_{||}$ value of 2.33, somewhat similar behavior of our study. We are currently on investigation of the *in vitro* anticancer activities of the present set of ligands and complexes.

Acknowledgements

E. Manoj thanks the University Grants Commission, New Delhi, India, for the financial support. M.R.P. Kurup is thankful to the CSIR, New Delhi, India, for the financial support.

Appendix A. Supplementary data

Supplementary data associated with this article can be found, in the online version, at doi:10.1016/j.saa.2008.10.030.

References

[1] O. Khan, Angew. Chem. Int. Ed. Engl. 24 (1985) 834.
[2] B. Moubaraki, K.S. Murray, J.D. Ranford, X. Wang, Y. Xu, Chem. Commun. (1998) 353.
[3] C. He, C.-y. Duan, C.-j. Fang, Y.-j. Liu, Q.-j. Meng, J. Chem. Soc., Dalton Trans. (2000) 1207.
[4] A. Bacchi, A. Bonini, M. Carcelli, F.J. Farraro, J. Chem. Soc., Dalton Trans. (1996) 2699.
[5] A. Bacchi, M. Carcelli, P. Pelagatti, C. Pelizzi, G. Pelizzi, F. Zani, J. Inorg. Biochem. 75 (1999) 123.
[6] B. Moubaraki, K.S. Murray, J.D. Ranford, J.J. Vittal, X. Wang, Y. Xu, J. Chem. Soc., Dalton Trans. (1999) 3573.
[7] R.C. DeConti, B.R. Toftness, K.C. Agarwal, R. Tomchick, J.A. Mead, J.R. Bertino, A.C. Sartorelly, W.A. Creasey, Cancer Res. 32 (1972) 1455.
[8] L.A. Saryan, E. Ankel, C. Krishnamurti, D.H. Petering, H. Elford, J. Med. Chem. 22 (1979) 1218.
[9] E. Manoj, M.R.P. Kurup, H.-K. Fun, Inorg. Chem. Commun. 10 (2007) 324.
[10] E. Manoj, M.R.P. Kurup, H.-K. Fun, S. Chantrapromma, Acta Cryst. E61 (2005) o4110.
[11] E. Manoj, M.R.P. Kurup, E. Suresh, J. Chem. Cryst. 38 (2008) 157.
[12] E. Manoj, M.R.P. Kurup, H.-K. Fun, A. Punnoose, Polyhedron 26 (2007) 4451.
[13] U.L. Kala, S. Suma, M.R.P. Kurup, S. Krishnan, R.P. John, Polyhedron 26 (2007) 1427.
[14] K. Nakamoto, Infrared and Raman spectra of Inorganic and Coordination Compounds, 5th ed., Wiley, New York, 1997.
[15] R.J. Clark, C.S. Williams, Inorg. Chem. 4 (1965) 350.
[16] A.M. Bond, R.L. Martin, Coord. Chem. Rev. 54 (1984) 23.
[17] P.F. Rapheal, E. Manoj, M.R.P. Kurup, Polyhedron 26 (2007) 818.
[18] A. Sreekanth, M.R.P. Kurup, Polyhedron 22 (2003) 3321.
[19] M. Joseph, M. Kuriakose, M.R.P. Kurup, E. Suresh, A. Kishore, S.G. Bhat, Polyhedron 25 (2006) 61.
[20] A.B.P. Lever, Inorganic Electronic Spectroscopy, 2nd ed., Elsevier, Science Publishing Company, Amsterdam, 1984.
[21] B. Bleaney, K. Bowers, Proc. R. Soc. Lond. Sect. A 214 (1952) 451.
[22] W.A. Alves, R.H.A. Santos, A. Paduan-Filho, C.C. Becerra, A.C. Borin, A.M.D.C. Ferreira, Inorg. Chim. Acta 357 (2004) 2269.
[23] B. Viossat, F.T. Greenaway, G. Morgant, J.-C. Daran, N.-H. Dung, J.R.J. Sorenson, J. Inorg. Biochem. 99 (2005) 355.
[24] D. Kivelson, R. Neiman, J. Chem. Phys. 35 (1961) 149.
[25] A.L. van den Brenk, J.D.A. Tyndall, R.M. Cusack, A. Jones, D.P. Fairlie, L.R. Gahan, G.R. Hanson, J. Inorg. Biochem. 98 (2004) 1857.
[26] R. Cejudo, G. Alzuet, M. Gonzalez-Alvarez, J.L. Garcia-Gimenez, J. Borras, M. Liu-Gonzalez, J. Inorg. Biochem. 100 (2006) 70.
[27] S. Stoll, A. Schweiger, J. Mag. Res. 178 (2006) 42.
[28] V. Uma, M. Kanthimathi, J. Subramanian, B.U. Nair, Biochim. Biophys. Acta 1760 (2006) 814.
[29] B.J. Hathaway, D.E. Billing, Coord. Chem. Rev. 5 (1970) 143.
[30] P. Peisach, W.E. Blumberg, Arch. Biochem. Biophys. 165 (1974) 691.
[31] U. Sakaguchi, A.W. Addison, J. Chem. Soc., Dalton Trans. (1979) 600.
[32] R. Pogni, M.C. Bartto, A. Diaz, R. Basosi, J. Inorg. Biochem. 79 (2000) 333.
[33] A. Rockenbauer, J. Magn. Reson. 35 (1979) 429.
[34] T.D. Smith, J.R. Pilbrow, Coord. Chem. Rev. 13 (1974) 173.
[35] B.J. Hathaway, in: G. Wilkinson, R.D. Gillard, J.A. McCleverty (Eds.), Comprehensive Coordination Chemistry II, vol. 5, Pergamon, Oxford, 1987, p. 533.
[36] A.H. Maki, B.R. McGravey, J. Chem. Phys. 28 (1958) 35.